

Short Report

Fabrication of Perovskite Solar Cells by the Smart Stacking ProcessMikhail Pylnev ^{1,*}, Hussain Al-Awadhi ^{1,2}, Nouar Tabet ^{1,2,*}

1. Center for Advanced Materials Research (CAMR), Research Institute of Sciences and Engineering, University of Sharjah, United Arab Emirates; E-Mails: mpylnev@sharjah.ac.ae; halawadhi@sharjah.ac.ae; ntabet@sharjah.ac.ae
2. Dept. of Applied Physics and Astronomy, University of Sharjah, United Arab Emirates

* **Correspondences:** Mikhail Pylnev and Nouar Tabet; E-Mails: mpylnev@sharjah.ac.ae; ntabet@sharjah.ac.ae

Academic Editor: Mohammad Jafari**Special Issue:** [Optimal Energy Management and Control of Renewable Energy Systems](#)

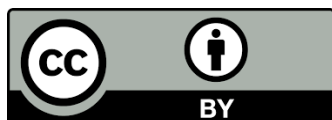
Journal of Energy and Power Technology
2022, volume 4, issue 4
doi:10.21926/jept.2204038

Received: September 21, 2022**Accepted:** November 20, 2022**Published:** November 25, 2022**Abstract**

The most commonly used process for fabricating perovskite solar cells is based on wet chemistry, which greatly limits the choice of materials suitable for optimizing the performance of the device. We developed a new approach for the fabrication of perovskite-based solar cells. In the smart stacking process, the perovskite solar cell was assembled by stacking two pieces of perovskite films prepared separately. A working perovskite solar cell was developed with PCE = 0.78% and the perovskite layer was analyzed with XRD and SEM. Our findings showed new ways to address some of the major fabrication challenges associated with the commercialization of perovskite solar cells.

Keywords

PSC; stacking process; encapsulation



© 2022 by the author. This is an open access article distributed under the conditions of the [Creative Commons by Attribution License](#), which permits unrestricted use, distribution, and reproduction in any medium or format, provided the original work is correctly cited.

1. Introduction

Organic-inorganic lead halide perovskite material-based solar cells (PSCs) are affordable and relatively easy to manufacture. They possess unique intrinsic properties like broad absorption spectra, fast charge separation, long diffusion distance of charge carriers, and long carrier separation lifetime, which ensure high power conversion efficiency (the highest efficiency recorded is 25.7%). This makes PSCs favorable for providing inexpensive solar electricity. However, several limitations hinder the mass production of PSCs, including 1) the high price of the electrode material (gold) and the hole-transporting material (Spiro-OMeTAD); 2) degradation of the perovskite absorber in the air due to the presence of moisture; 3) inability to use high-temperature regimes for the layers above the perovskite absorber since the perovskite materials decompose at relatively low temperatures.

All traditional ways of preparing perovskite solar cells require the sequential deposition of the functional layers of the device. A perovskite solar cell consists of a transparent conductive oxide layer on glass, an electron transporting layer (ETL), a perovskite absorber layer, a hole-transporting layer (HTL), and gold contacts. The most-commonly used HTL is Spiro-OMeTAD, which is costly and requires overnight oxidation, and leads to low reproducibility of the PSC device [1]. Inorganic HTL solutions were used in some studies, but they require high annealing temperatures of $\sim 400^{\circ}\text{C}$ [2], while perovskites decompose at temperatures below 300°C [3]. Thus, inorganic HTLs suit inverted PSCs with the p-i-n configuration. However, in this configuration, the ETL layer must be prepared by a low-temperature technique that is compatible with deposition in a dry environment [4, 5]. Thus, in the sequential deposition process, one of the charge-transporting layers must be prepared at a low temperature.

In this manuscript, a new approach, called “smart stacking” was introduced. The method was first described in a patent [6]; however, a prototype was not described. The Smart Stacking Process (SMS) allows separate preparation of the hole-transporting and electron-transporting layers and the use of high-temperature processes for both layers. This eliminates any restriction for the temperature regime and the choice of charge transporting layers.

It also encapsulates the PSC during fabrication. The new SMS process significantly decreases the cost of the device by replacing the unstable organic HTL and the gold contacts with inorganic HTL and a transparent conducting oxide (TCO), respectively.

2. Materials and Methods

2.1 Smart Stacking Process

In the SMS process, the perovskite solar cell was assembled by stacking charge-transporting layers with perovskite precursor films. The ETL was planar and prepared as follows. A schematic representation of the SMS process is shown in Figure 1a. First, a $2 \times 2 \text{ cm}^2$ piece of fluorine-doped tin oxide (FTO) ($10 \Omega/\text{sq}$, NSG, Japan) was etched with HCl and Zn to create a pattern of a small stripe of FTO $\sim 0.7 \text{ cm}$ in the center leaving the bare glass on the sides to prevent short circuits in the device. Then, the ETL layer consisting of TiO_2 and SnO_2 was deposited. The first layer of ETL, consisting of TiO_2 ($\sim 50 \text{ nm}$), was spin-coated using an ethanol solution (99.9%; Sigma-Aldrich, US) containing 0.2 M titanium diisopropoxide bis (acetylacetonate) in 2-propanol (99.9%; Sigma-Aldrich, US) at 4,000 rpm for 20 s and 8,000 rpm for 10 s followed by annealing at 500°C for 1 h.

Next, the second layer of the ETL, consisting of SnO_2 , was spin-coated using an aqueous solution of 0.075 M $\text{SnCl}_4 \cdot 5\text{H}_2\text{O}$ (98%; Sigma-Aldrich, US) at 3,000 rpm for 30 s. Then, the samples were annealed at 180°C for 1 h.

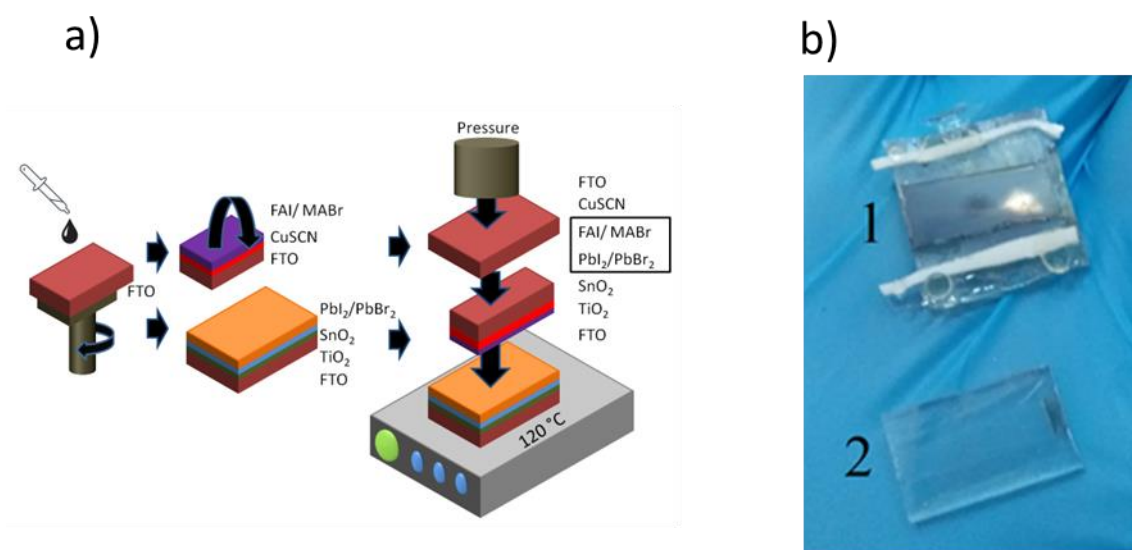


Figure 1 a) A schematic representation of the smart stacking process; b) stacked PSCs with exposed FTO electrodes: 1- ETL piece; 2- HTL piece.

The HTL piece was prepared as follows. A film of CuSCN was deposited on a piece of $1 \times 1 \text{ cm}^2$ FTO by dynamically dispensing 50 μL of its solution (30 mg/mL) CuSCN (99%, Sigma-Aldrich, US) in diethyl sulfide (98%, Sigma-Aldrich, US) on a substrate using a spin-coater at 6,000 rpm. Then, the films were annealed at 80°C for 10 min.

On the piece of ETL, the porous $\text{PbBr}_2/\text{PbI}_2$ layer was deposited by spin-coating at 2,000 rpm for 20 s solution containing 705.33 mg of PbI_2 (99.99%; Xi'an Polymer Light Technology Corporation, China) and 40.37 mg of PbBr_2 (99.999%; Sigma-Aldrich, US) in 1 mL of a mixture of DMF (dried 99.9%; MERCK) (80 v%) and DMSO (anhydrous, $\geq 99.9\%$; Sigma-Aldrich, US) (20 v%). To obtain a porous structure, the film was immersed for 10 s in isopropyl alcohol (99.9% Sigma-Aldrich, US) and dried at 6,000 rpm for 30 s. Then, the film was annealed at 70°C for 10 min.

After preparing the ETL and HTL layers, the organic part of the perovskite precursor was spin-coated on both pieces at 2,000 rpm for 30 s. The solution had 240.4 mg of FAI (Greatcell solar, Australia), 33.76 mg of MACl (Lumtec, Taiwan), and 12.32 mg of MABr (Greatcell solar, Australia) in 2 mL of isopropyl alcohol.

Subsequently, the layers were scratched from the ETL piece up to the etched central part and small plastic stripes were placed on the edges of the $2 \times 2 \text{ cm}^2$ piece to protect the central part from epoxy, as shown in Figure 1b.

Finally, the ETL and HTL pieces were stacked on each other. Then, a piece of glass $2 \times 2 \text{ cm}^2$ was put on top of them and pressure was applied to the whole setup using the rods of a pressing device.

The pieces were glued using Liquid Plastic Welder “Bondic” (Rob Harbauer, Germany) and the pieces were annealed under the pressure of the rods at 120°C for 1.5 h. The SMS-made disassembled cell is shown in Figure 1b.

2.2 Measurements

A scanning electron microscope (SEM) VEGA4 XM SEM (TESCAN) was used to observe the morphological characteristics of the layers. The XRD patterns of the samples were recorded using the X-ray Diffractometer (XRD) Bruker D8 ADVANCE system with a Cu anode. For the analysis, the ETL/HTL pieces of a stacked PSC were dismantled. The relationship between current density and voltage (J-V) of the PSCs was measured using a solar simulator (SunLite Solar Simulator model 11002, Abet Technologies) with a computer-controlled digital source meter (X-200 Ossila, UK). The measurements were recorded under a 100 mWcm² irradiance of the AM1.5G spectrum.

3. Results and Discussion

Perovskite solar cells were first described by the smart stacking process (SMS) in patent [6]. Although the study did not describe a prototype, it explained how the perovskite layer can form through chemical reactions when two pieces containing organic and inorganic precursor films of the perovskite MAPbI₃ come in contact. Several differences occurred between the design in [6] and our study. First, we used FTO as both the cathode and anode. Our design also included the sealing of the device. Our HTL piece consisted of FTO/CuSCN/(FAI-MABr-MACI), while the ETL piece consisted of FTO/TiO₂/SnO₂/(PbBr₂-PbI₂)/(FAI-MABr-MACI).

We modified several steps in the process described in [6] to make a working photovoltaic cell.

First, obtaining uniform perovskite precursor layers on both ETL and HTL pieces is important. While the ETL consisting of TiO₂ and SnO₂ had no issues with wettability by the inorganic precursor, the organic precursor did not wet the other HTLs we used, including MoO₃, NiO, PEDOT: PSS, and P3HT. However, CuSCN facilitated a flawless deposition of the metal-organic perovskite precursor.

Second, we followed the method described in the patent [6] and stacked the FTO/ETL/(FAI/MABr/MACI) and FTO/ETL(PbBr₂/PbI₂) layers. The samples under pressure were annealed at 120°C for 1.5 h. The results of XRD analysis of the perovskite layer formed in this stack are shown in Figure 2 (“planar inorganic layer”). The density of PbI₂ is around 1.5 times more than the density of MAPbI₃. Thus, the growing perovskite layer expanded [7]. After a thin dense layer formed on the surface of PbI₂, it further decreased the penetration of MAI; thus, leaving a substantial amount of PbI₂ unreacted [8].

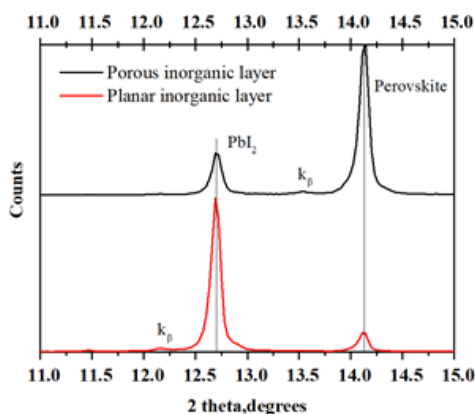


Figure 2 The XRD patterns of SMS PSCs prepared using planar and porous inorganic precursors

We used the mediator extraction treatment in which a pre-deposited DMSO-PbI₂ complex film was converted into a porous film by rinsing it with IPA. The transparent inorganic film turned hazy within a few seconds. This caused the inorganic film to form a porous structure and the PbI₂ crystallites to have a random orientation [9]. Thus, the film was porous and could accommodate more MAI. The porous structure of PbI₂/PbBr₂ is shown in Figure 3a.

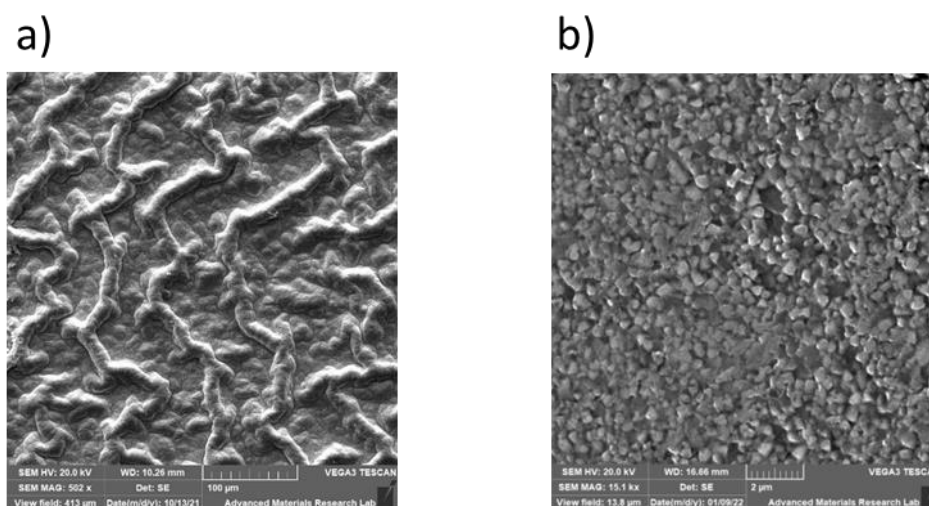


Figure 3 The SEM images of a) a porous PbI₂/PbBr₂ film; b) a perovskite film produced by the SMS process.

Next, stacking the inorganic and organic parts of the perovskite precursor did not provide a working photovoltaic cell (the photocurrent was zero). This was due to poor contact between the two pieces. Thus, the precursor organic films of halved concentrations were deposited on both pieces, i.e., the bare HTL piece and the ETL piece with the porous inorganic precursor film. This method ensured contact between the organic films of the same composition, leading to a chemical connection between the pieces.

Another challenge that we encountered regarding deposition in the SMS process was the sealing of the device with epoxy, which can protect the device from moisture and ensure close contact between the ETL and HTL pieces. Upon heating, epoxy went between the pieces before pressure could be applied and isolated the device. To avoid this problem, we pressed the ETL and HTL pieces with an additional piece of FTO (see Experimental procedure) at room temperature, after which we started the heating process.

The annealing temperature we used for the SMS process also differed from the annealing temperature used for the perovskite formula [10]. When we annealed it at temperatures higher than 120°C, the device turned yellow, which indicated evaporation of the organic part. This might be associated with the pressure applied to the stacked device. Prolonged annealing at 120°C resulted in a good perovskite/PbI₂ ratio, as determined from the XRD pattern (Figure 2).

In this study, we designed the first working cell prepared by the smart stacking (SMS) process. The J-V curves of the SMS- perovskite solar cells are shown in Figure 4.

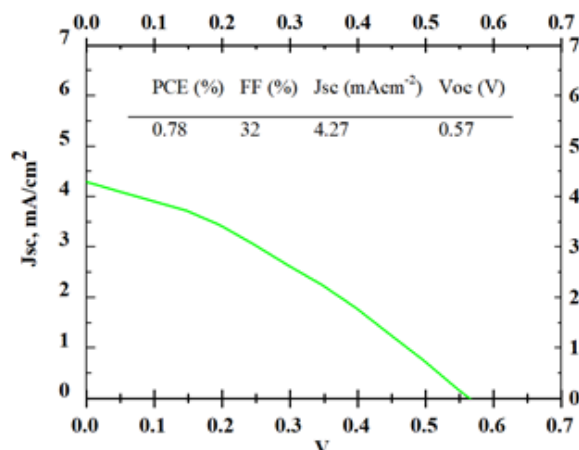


Figure 4 The J-V curves of the perovskite solar cells prepared by the smart stacking method

The Open-circuit voltage (Voc) and Fill Factor (FF) were relatively low because of the poor interface between the layers and poor morphology of the perovskite, as determined from the SEM images (Figure 3b). The obtained PCE of 0.78% showed that the photovoltaic cell was functional and the approach was favorable.

Our method had some advantages over the standard method of producing PSCs, which include:

- 1) The possibility to prepare separate hole-transporting and electron-transporting layers for PSCs, which can facilitate high-temperature treatments for both layers.
- 2) The new process did not require gold or spiro-OMeTAD, which generally contribute up to 30% of the total cost of fabrication of PSCs [11].

4. Conclusions

A new approach for the fabrication of perovskite-based solar cells was developed. Based on the smart stacking process, a perovskite solar cell was assembled by stacking electron-transporting layers and hole-transporting layers with perovskite precursor films. A perovskite solar cell was produced and used, and the perovskite layer was analyzed by performing XRD and SEM analyses. Separate preparation of hole-transporting and electron-transporting layers for PSCs facilitated the application of high-temperature treatments for both layers. The new process excluded the use of organic HTL and gold and, thus, reducing the cost of producing a PSC substantially. Encapsulation of the perovskite solar cells was performed during the smart stacking process, which ensured stable operation under ambient conditions.

Author Contributions

Mikhail Pylnev- experiments, optimization, initial draft; Hussain Al-Awadhi-supervision, Nouar Tabet- initial idea, supervision; all authors contributed to discussion of the manuscript.

Funding

The authors would like to acknowledge the financial support from the University of Sharjah (Project# 2102143098).

Competing Interests

The authors have declared that no competing interests exist.

References

1. Guo Y. A novel organic dopant for Spiro-OMeTAD in high-efficiency and stable perovskite solar cells. *Front Chem.* 2022; 722: 928712. doi: 10.3389/fchem.2022.928712.
2. Khan F, Rezgui BD, Kim JH. Analysis of PV cell parameters of solution processed Cu-doped nickel oxide hole transporting layer-based organic-inorganic perovskite solar cells. *Sol Energy.* 2020; 209: 226-234. doi: 10.1016/j.solener.2020.09.007.
3. Ranjan R, Ranjan S, Monalisa M, Nalwa KS, Singh A, Garg A, et al. Enhanced thermal and moisture stability via dual additives approach in methylammonium lead iodide based planar perovskite solar cells. *Sol Energy.* 2021; 225: 200-210. doi: 10.1016/j.solener.2021.06.076.
4. Khan F, Kim JH. Enhanced charge-transportation properties of low-temperature processed Al-doped ZnO and its impact on PV cell parameters of organic-inorganic perovskite solar cells. *Solid State Electron.* 2020; 164: 107714. doi: 10.1016/j.sse.2019.107714.
5. Khan F, Khan MT, Rehman S, Al-Sulaiman F. Analysis of electrical parameters of pin perovskites solar cells during passivation via N-doped graphene quantum dots. *Surf Interfaces.* 2022; 31: 102066. doi: 10.1016/j.surf.2022.102066.
6. Matthew R, Alex G. Fabrication of stacked perovskite structures. Berkeley, CA: Energy Everywhere, Inc.; 2018; WO2019074616A2.
7. Zhang T, Yang M, Zhao Y, Zhu K. Controllable sequential deposition of planar $\text{CH}_3\text{NH}_3\text{PbI}_3$ perovskite films via adjustable volume expansion. *Nano Lett.* 2015; 15: 3959-3963. doi: 10.1021/acs.nanolett.5b00843.
8. Kwang ZW, Chang CW, Hsieh TY, Wei TC, Lu SY. Solvent-modulated reaction between mesoporous PbI_2 film and $\text{CH}_3\text{NH}_3\text{I}$ for enhancement of photovoltaic performances of perovskite solar cells. *Electrochim Acta.* 2018; 266: 118-129. doi: 10.1016/j.electacta.2018.02.026.
9. Kim YY, Park EY, Yang TY, Noh JH, Shin TJ, Jeon NJ, et al. Fast two-step deposition of perovskite via mediator extraction treatment for large-area, high-performance perovskite solar cells. *J Mater Chem A.* 2018; 6: 12447-12454. doi: 10.1039/C8TA02868K.
10. Gao C, Shao Z, Sun X, Li Z, Rao Y, Lv P, et al. Fabrication and Characterization of $\text{FA}_x\text{Cs}_{1-x}\text{PbI}_3$ Polycrystal Perovskite Solar Cells. *Sol RRL.* 2021; 5: 2100166. doi:10.1002/solr.202100166.
11. Yang F, Wang S, Dai P, Chen L, Wakamiya A, Matsuda K. Progress in recycling organic-inorganic perovskite solar cells for eco-friendly fabrication. *J Mater Chem A.* 2021; 9: 2612-2627. doi: 10.1039/D0TA07495K.



Enjoy *JEPT* by:

1. [Submitting a manuscript](#)
2. [Joining in volunteer reviewer bank](#)
3. [Joining Editorial Board](#)
4. [Guest editing a special issue](#)

For more details, please visit:

<http://www.lidsen.com/journal/jept>